# DAMAGE DETECTION IN CONCRETE BEAMS UNDER IMPACT LOAD USING PIEZO SENSORS

A DISSERTATION
SUBMITTED IN PARTIAL FULFILLMENT OF THE REQUIREMENTS
FOR THE AWARD OF DEGREE
OF

MASTER OF TECHNOLOGY

IN

**STRUCTURAL ENGINEERING**


Submitted by

**ARYA SAJITH**

**2K20/STE/05**

Under the supervision of

**Dr. SHILPA PAL**

**(Associate Professor)**




**DEPARTMENT OF CIVIL ENGINEERING**
DELHI TECHNOLOGICAL UNIVERISTY
(formerly Delhi College of Engineering)
Bawana Road, Delhi - 110042


**MAY, 2022**

**DEPARTMENT OF CIVIL ENGINEERING**
DELHI TECHNOLOGICAL UNIVERISTY
(formerly Delhi College of Engineering)
Bawana Road, Delhi - 110042

# CANDIDATE'S DECLARATION

I, ARYA SAJITH , 2K20/STE/05, student of M.Tech ( Structural Engineering), hereby declare that the project Dissertation titled "**Damage detection in concrete beams under impact load using piezo sensors**" which is submitted by me to the Department of Civil Engineering, Delhi Technological University, Delhi in partial fulfilment of the requirement for the award of the degree of Master of Technology, is original and not copied from any source without proper citation. This work has not previously formed the basis for award of any Degree, Diploma Associateship, Fellowship or other similar title or recognition.

Place : Delhi **ARYA SAJITH**

Date: 30-05-2022

**DEPARTMENT OF CIVIL ENGINEERING**
DELHI TECHNOLOGICAL UNIVERISTY
(formerly Delhi College of Engineering)
Bawana Road, Delhi – 110042

# CERTIFICATE

I hereby certify that the Project Dissertation titled "Damage detection in concrete beams under impact load using piezo sensor" which is submitted by ARYA SAJITH , 2K20/STE/05, Department of Civil Engineering, Delhi Technological University, Delhi in partial fulfilment of the requirement for the award of the degree of Master of Technology, is a record of the project work carried out by the student under my supervision. To the best of my knowledge, this work has not been submitted in part or full for any Degree or Diploma to this University or elsewhere.

Place: Delhi

Date: 30-05-2022

**Dr. SHILPA PAL**

SUPERVISOR
Associate professor
Department of Civil Engineering
Delhi Technological University
Bawana road, Delhi - 110042

# ABSTRACT

Over the past few years, damage detection and structural health monitoring has gained a lot of interest in the civil engineering field. It helps in analysing a system over a period of time by monitoring their changes in properties like geometrical or material, of engineering various structures.

Smart materials such as lead zirconate titanate (PZT) is being widely used to detect damages in a structure with the help of electro-mechanical impedance (EMI) technique. The PZT patches uses high frequency responses to detect damage. The EMI technique uses both the direct and converse piezoelectric effect which allows the PZT sensor to act as both the actuator and the sensor. Changes in admittance signature indicates the damage and this is quantified by using root mean square deviation index (RMSD).

In this study, damage detection of plain concrete beams with embedded PZT sensors under impact load are used to find the extent of damage detection properties of PZT sensors. Parametric study on height of impact, position of sensors and grade of concrete has also been done. This is further validated with the help of ANSYS software through finite element analysis. For this, velocity impact simulations have been done in ANSYS Explicit dynamics module and the behaviour of the concrete beams have been studied. From the study, it can be concluded that the RMSD percentage value and peak value of admittance signature is increasing with each impact which indicates the increase in extent of damage.. It can be concluded that EMI technique has proven to be one of the effective methods for structural health monitoring and in detecting damages.

# ACKNOWLEDGEMENT

I would like to express my sincere gratitude to my supervisor **Dr. Shilpa Pal** (Associate professor, Delhi Technological University) for the continuous support for my MTech study and research, for her patience, motivation and guidance. I am thankful to **Prof. V K Minocha** (Head of the Department, Delhi technological university) and **Prof. Alok Verma** (Professor, Delhi technological university) for providing me the facilities for my experiment in the concrete lab.

I extend my heartiest gratitude to **Mr. Indrajeet Singh** ( PhD Scholar, Delhi Technological University) for his constant support and help throughout my work. I am thankful to all the lab assistants of concrete lab, DTU for their help during my experimental work. I am sincerely thankful to all the teachers who have ever taught me, who gave me strength, courage and knowledge to reach where I am.

I have no words to express my appreciation for the unbound love and support from my family and friends who have helped me to overcome any obstacles during the course of my work.

ARYA SAJITH

# TABLE OF CONTENTS

# LIST OF TABLES

# LIST OF FIGURES

# ABBREVIATIONS

| Abbreviation | Description |
|---|---|
| EMI | Electro – mechanical impedance |
| PZT | Lead zirconate titanate |
| NDT | Non- destructive evaluation technique |
| FEM | Finite element modelling |
| ACI | American concrete institute |
| IS | Indian standards |
| RMSD | Root mean square deviation |
| MAPD | Mean absolute percentage deviation |
| PPC | Portland pozzolana cement |

# CHAPTER 1

# INTRODUCTION

## 1.1 BACKGROUND

Structures undergo a number of changes in their life time. With passage of time, flaws and faults are bound to happen in any structure due to a number of reasons, let it be environmental exposure or natural causes like earthquake or extreme loads like wind [22].Monitoring and assessment of performance of structures is very important to avoid catastrophic failure[20]. Early detection of damages is necessary for rehabilitation and retrofitting of damaged structure as well.

Visual inspection was the primary mode of monitoring used to find damages in a structure[2]. An experienced personal does the assessment and later on localised damages are further analysed with the help of other non-destructive evaluation techniques (NDE) like ultrasound , magnetic particle inspection or eddy-current testing to get a detailed assessment. But visual inspections are un-reliable and tedious. It depends completely on the opinion of the trained personal. Critical and incipient damages might not even be recognised through these procedure which could ultimately lead to failure of the structure. Moreover, most NDE techniques requires to know the exact location of damage which might not be possible all the time[2]. Unattended structural damage can grow and can lead to reduction in load carrying capacity , increase in vibration etc [20]. Rehabilitation of such structures will lead to highly expensive methods of strengthening.

This is where a continuous monitoring comes into play. Many researchers have been studying for the scope of continuous structural health monitoring for two decades. Use of smart materials in structural health monitoring for damage detection have been

explored by researchers. This will ensure a proper maintenance and early detection of damages in structures which can help in strengthening of them.

## 1.2 SMART MATERIALS – PIEZOELECTRIC TRANSDUCER

Smart materials are materials in which one or more properties can be altered or controlled by some external stimuli, like stress, temperature, light etc. They have the capability for sensing any changes in the environment like electrical, geometrical etc[1]. and give an accurate response to it. There are wide range of smart materials where each material changes different properties like photovoltaic materials, magnetic shape memory, chromogenic materials, piezoelectric materials etc . Among these, piezo electric materials are the most widely used smart material for structural health monitoring.

Piezo electricity is the phenomenon where there is a coupling action between the mechanical and electrical properties of the material i.e., mechanical energy gets converted into electrical energy and electrical energy into mechanical energy. Piezo electric ceramic transducers ( lead zirconate titanate) also known as PZT falls comes under this category. Their ability to create an electric field or electric charge when a mechanical stress acts on them is known as direct effect and alternatively a mechanical strain or geometrical deformation is developed when an electric field is applied to it which is known as the converse effect. This dual effect of piezo electric transducers are the highlight of these patches as this allow them to act as both sensors and actuators. The direct effect allows them to be used as a sensor and the inverse or converse effect allows them to be used as the actuators.

When a sensor is exposed to mechanical stress, it will generate a charge proportional to the stress in response. The actuator which is bonded with the structure, on the other hand, when applied an electric charge, it will generate a mechanical induced deformation.

As per Bhalla (2004) , the direct and converse effect can be represented as the following equations (1.1) and (1.2) for small field conditions.

$$D_i = \bar{\varepsilon}_{ij}^{T} E_j + d_{im}^{d} T_m \quad (1.1)$$

$$S_k = d_{jk}^{c} E_j + \bar{s}_{km}^{E} T_m \quad (1.2)$$

Where electrical displacement is represented by $D_i$ showing the direct effect and the mechanical strain is represented by $S_k$ showing the converse effect. $E_j$ is representing the applied electric field , $T_m$ is representing the stress, $\bar{\varepsilon}_{ij}^{T}$ and $\bar{s}_{km}^{E}$ represents the electric permittivity and elastic compliance under constant stress and electric field respectively and $d_{im}^{d}$ and $d_{jk}^{c}$ are piezoelectric strain constants where i, j and m,k represent the direction of electric field and strain respectively[16].

Assuming the host structure to be a skeletal structure as in ig. 1.1, one dimensional interaction between the PZT patch and the host structure was considered.

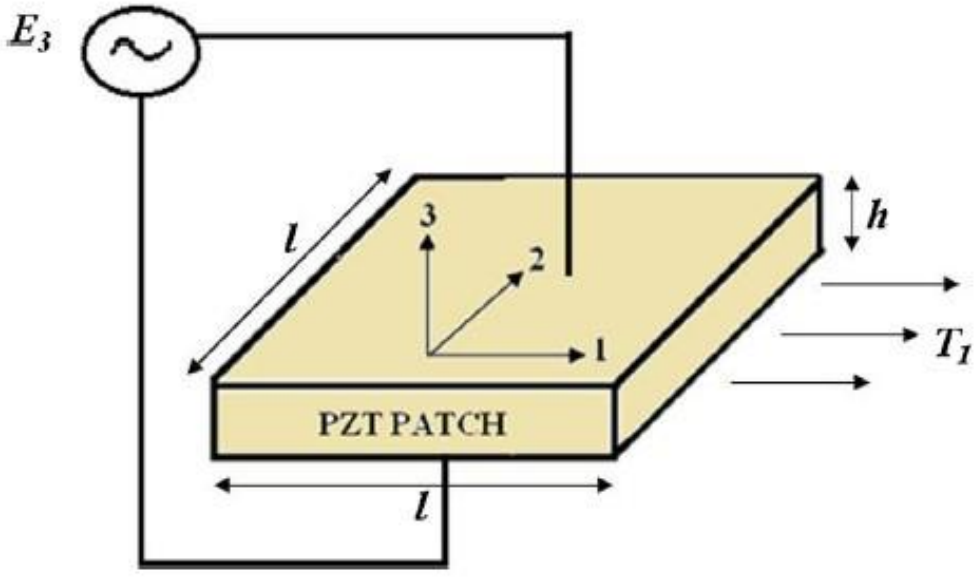


**Fig 1.1** 1D interaction of PZT patch under stress and electric field[1]

Considering the 1D interaction, the above equation are simplified as the following:

$$D_3 = \overline{\varepsilon_{33}^T}\, E_3 + d_{31} T_1 \tag{1.3}$$

$$S_1 = \frac{T_1}{\overline{Y^E}} + d_{31} E_3 \tag{1.4}$$

Where $\overline{\varepsilon_{33}^T}$ and $\overline{Y^E}$ represents the complex electric permittivity ( in direction 3) and young's modulus of elasticity under constant stress and electric field respectively[16].

Based on these equations, another relation was developed between the voltage generated across the PZT and the strain developed in the host structure by shanker et al and it is given as:

$$V = \left(\frac{d_{31}\overline{Y^E} h}{\overline{\varepsilon_{33}^T}}\right) S_1 \tag{1.5}$$

here, V is the output voltage. From the above equation, strain can be calculated by substituting the value of V that is obtained by using an oscilloscope and connecting it to the PZT patch [14].

## 1.3 ELECTRO-MECHANICAL IMPEDANCE TECHNIQUE

In electro-mechanical impedance or EMI technique, PZT patches acts as transducers in detecting damages. The damage is detected by measuring the admittance signature of the PZT patch that is bonded to the structure. The highlight of the EMI technique is the high frequency range that it uses which separates this technique from all other.

In EMI based technique, the PZT patches can be bonded with structure in three ways- non bonded, surface bonded and embedded[3] . These are bonded using highly adhesive epoxy resins. It works on both direct and converse piezoelectric effect. LCR meter is a device used to record the vibration response. This LCR meter excites the piezo patches attached on the structure at high frequency varying in a range from 30 – 500 KHz [2].

This causes the PZT patches to produce mechanical strain or vibrations i.e., due to the excitation**,** a strain will be developed in the structure. Hence the PZT patch acts as an actuator in this case. Now acting as a sensor, the patch receives a signal back which consists of structural properties and this is called an admittance signature. These admittance signatures are very unique to each structure. It consists of a real part called conductance and an imaginary part called inductance. Any change or damage in structure will alter the admittance signature thereby indicating damage in the structure. The admittance signature is altered because when the structure has a damage , it affects the mechanical impedance which is essentially a function of stiffness, mass and damping of the structure [17].

Liang et al [4] found out a relation between the electrical and structural impedance for one dimensional PZT patches. This was later extended for 2 D by Bhalla and Soh [17] and expressed the admittance $\bar{Y}$ in ohms as equation (1.6).

$$\bar{Y} = G + Bj = 4\omega\frac{l^2}{h}\left(\varepsilon_{33}^{\bar{T}} - \frac{2d_{31}^2\overline{Y^E}}{1-\nu}\right) + \frac{8\omega d_{31}^2\overline{Y^E}l^2}{h(1-\nu)}\left(\frac{Z_{a,eff}}{Z_{s,eff}+Z_{a,eff}}\right)\bar{T}\ \mathrm{j} \qquad (1.6)$$

Where, G is conductance, B is the susceptance, x is the angular frequency, $Z_{a,eff}$ and $Z_{s,eff}$ are the mechanical impedance of PZT patch and host structure respectively.$\overline{Y^E}$ is the Young's modulus and $\varepsilon_{33}^{\bar{T}}$ is the electric permittivity of the patch, l and h are length and thickness of PZT patch ,$d_{31}$ is the piezoelectric strain coefficient, $\nu$ is the Poisson's ratio of the PZT patch and $\bar{T}$ is the tangent ratio and it is given as equation (1.7).

$$\bar{T} = \frac{1}{2}\left(\frac{\tan C_1 kl}{C_1 kl} + \frac{\tan C_2 kl}{C_2 kl}\right);\ k = \omega\sqrt{\frac{\rho(1-\nu^2)}{\overline{Y^E}}} \qquad (1.7)$$

Where , $k$ is the wave number and ω is the density of the PZT patch.

When a structure undergoes any damage, the parameters like stiffness, mass distribution etc changes, which changes the impedance of the host structure. But the parameters

associated with PZT will remain unchanged, so the electro- mechanical admittance recorded will undergo a change which can be considered as a measure of indicator of the health of the structure. The real part of the signature i.e., the conductance interacts the most with the structure and the imaginary part has very weak interaction, hence all the studies so far has taken the real part into consideration while doing the analysis. The imaginary part of the signature can be used to make sure that the PZT patch is bonded with the structure throughout.

## 1.4. OBJECTIVES OF THE STUDY

The main objectives of this study is as follows:

- To experimentally investigate the capability of piezo sensors in damage detection under impact load using EMI technique on concrete beam.
- To analyse the damage detection property of sensors under impact load for different parameters.
- Validation of experimental work with analytical work using ANSYS software.
- To use statistical techniques to quantify the damage detection ability of piezo sensor .

## 1.5 ORGANIZATION OF THESIS

**Chapter 1 -** deals with the description about an introduction to the topic, its application and significance.

**Chapter 2-** discusses some of the literature and previous work on damage detection and piezo sensors.

**Chapter 3 –** discusses the methodology followed along with details of the experimental and analytical work carried out.

**Chapter 4 -** discusses the validation of the work with literature, the results and discussion related to damage detection using piezo sensors

**Chapter 5 –** deal with the conclusion of the present study and some suggestion for future work.

# CHAPTER 2

# LITERATURE REVIEW

## 2.1 GENERAL

This chapter involves the detailed literature study done in order to understand in depth about the working of piezo sensors and the electro mechanical impedance technique. Researches regarding the optimum orientation and location of piezo sensor along with the methods involved in quantifying the damage detection ability of piezo sensors have been studied and discussed below.

**Bhalla and Naidu (2003)** presented the ability of PZT transducers to detect damages that is even developed inside the concrete and is not visible to naked eye. It was shown that the detection of damage was not only on the surface where the PZT was bonded but also on the surface that is perpendicular to it. The extent of damage was quantified by analysing the increase in root mean square index deviation of the real part of admittance signature.

**Negi et al (2019)** studied for the effectiveness of four configuration of piezo sensors, namely concrete vibration sensor with circular and square patch and resin jacketed piezo sensor with single and double layer of resin. It was observed that all four configuration was successful in finding the damage but the circular patch concrete vibration senor and single layer resin jacketed sensor worked better in detecting damages by using root mean square deviation index method.

**Park et al (2000)** experimentally investigated the impedance based structural health monitoring and concluded that this technique was successful in detecting real time damages. They also tested the technique's capability under adverse environmental

conditions like variation in temperature and loads and it was proven that impedance based technique is very efficient in monitoring the condition of civil structures.

**Divsholi and Yang (2011)** discusses about the different ways in which the PZT transducers can be attached to the structure, namely surface bonded, embedded and reusable setup. EMI technique, wave transmission technique and wave propagation technique was studied for three types of bonding of the sensors. From the experimental study, it can be observed that embedded PZT were found to be effective in monitoring of hydration in concrete using both electro-mechanical impedance technique and wave propagation technique.

**Negi et al (2018)** studied the effect of different orientation of PZT patches namely 0˚, 45˚ and 90˚. The horizontal position (0˚) i.e., parallel to the structure's axis proved to be the most efficient orientation of the patch while performing the EMI technique. The inclined position of patch was least effective as it gave nearly flat response graph.

**Shanker et al (2011)** investigated the integration of EMI technique with the global dynamic technique for the health monitoring of civil structures. It was concluded that it is efficient and practical for finding incipient as well as severe damage. EMI technique has proven to be very efficient and sensitive to detect incipient damage but fails to distinguish the severe damages and this is where the global dynamic technique comes into play. They have also discussed about the relationship between voltage and strain of the PZT and structure.

**Duan et al (2010)** discusses about the efficiency of piezo electric sensors in structural health monitoring and repair. They explain in detail about the application of PZT patches in repair of structures by taking beams, pipes and plate elements as examples and the

techniques involved in it. They have also in detail discussed about the working of piezo electric materials.

**Bhalla and Soh (2004)** discusses in detail about the theoretical part of electro-mechanical impedance technique. They have formulated a new approach in order to model a connection between the piezo transducers and the host structure so as to extract the damage details or mechanical impedance from the admittance signature. The study also presents an analysis approach to find the structural parameters from the effective drive point impedance in order to detect damages in the host structure.

**Bhalla and Soh (2003)** presents a new approach to damage detection by extracting the mechanical impedance from the admittance signature of the PZT patches. The highlight of this method is the use of both real and imaginary part of the admittance signature to quantify the damage. The change in equivalent single degree of freedom damping caused by the damage is represented by the change in real part and the change in equivalent single degree of freedom stiffness-mass is represented by the change in imaginary part of the admittance signature.

**Fan et al (2018)** represents a relation between the damage volume ratio to the root mean square deviation index, which will compare it to the empirical value of the root mean square deviation index and predict the true degree of damage. It was observed from the study that there is a linear relationship between the damage ratio and the RMSD index which shows that the EMI technique is efficient in finding the impact damage .

**Pardo De Vero and Guemes (1998)** compared the self-sensing method of PZT to the cross talk method which is using separate sensor and actuator and validated the similarity of both the methods. It was also observed that the signal acquired during temperature

shifts has to be corrected with a scaling factor as the temperature change is changing the characteristics of PZT patches which shift the resonance frequency.

**Kaur et al (2018)** developed a system to detect damage and to monitor the retrofitting of structures using PZT sensors in the concrete vibrating sensor form. Natural frequency was used as the initial indicator and it was observed that there was a decrease in the value of natural frequency with increasing damage but it was found to be increasing again after retrofitting was done which indicates that the retrofitting helped in regaining the strength. The damage index was also another indicator which was found to increase with damage and then decrease after the retrofitting.

**Singh et al (2021)** focused on low and high-velocity impact simulations on reinforced concrete beam and slab to study the impact resistance of geopolymer reinforced concrete using finite element analysis. The study concluded that geopolymer concrete has better impact resistance compared to conventional concrete with the help of ANSYS simulations..

**Gayakwad et al (2022)** studied the effectiveness of structural health monitoring of piezo sensors by combining the electromechanical impedance technique and wave propagation technique. They have used smart sensing units to avoid the impact of vibration during casting on the PZT patch signatures. The combined technique was found to increase the PZT patch's effectiveness in detecting damage.

**Ai et al (2016)** did an experimental study on comparison of surface bonded PZT with embedded PZT patches and it was concluded that the durability and feasibility of the PZT patches are increased when they embedded as they are protected from any other environmental exposures and helps in filtering out the impact damage which will help in giving a more accurate result.

## 2.2 GAP OF THE STUDY

From the literature study, it was concluded that PZT patches are very much sensitive and use of EMI technique is very effective for detecting even the incipient damages. It was also observed that the embedded piezo sensors give out the good results as it is not disturbed by any other environmental factors or impact during vibration. Horizontal positioning of sensor were found to give better results compared to other orientation like 45˚ or 90˚.

There has been very few studies reported till date which studies the damage detection in plain concrete beams under impact loading as well as comparing its effect on different grades of concrete using piezo sensors.

# CHAPTER 3

# METHODOLOGY

## 3.1 GENERAL

A brief overview of the theoretical concepts of piezo sensors, EMI technique and damage detection using the PZT patches have been discussed in the earlier chapters. The objective of the present study to analyse the ability of piezo sensors to detect damages in concrete beams under impact load using EMI technique.

## 3.2 METHODOLODY

For attaining the objectives of the present study, the first step was to do a mix design for M30 grade concrete for casting the beams. After fixing the ratio, Plain concrete beam of size 700 x 150 x150mm was casted . The PZT patches were soldered and properly covered with epoxy resin. and they were kept embedded inside the concrete. Impact test was done using a spherical ball of 5kg in weight and dropped from a height of 2.5 m.

Parametric study on height of impact, grade of concrete, position of sensor was also done. The admittance signature of the sensors were taken before and after each impact. This will give us an understanding on how the peak changes with each impact. The oscilloscope was connected to the PZT patch during the testing of impact load and the voltage was measured throughout the impact. This voltage is later used to find out the strain that the PZT records during impact by using a formula mentioned by Sanker et al [14]. The rebound hammer test was also done to compare the health monitoring using NDE techniques and piezo sensors.

The beam with same dimension and impact load used in experimental work is modelled and simulated in ANSYS and the strain obtained from the software is compared with

strain to validate the experiment. RMSD and MAPD indexes are used to quantify the deviation of the signature from baseline and quantify the damage.

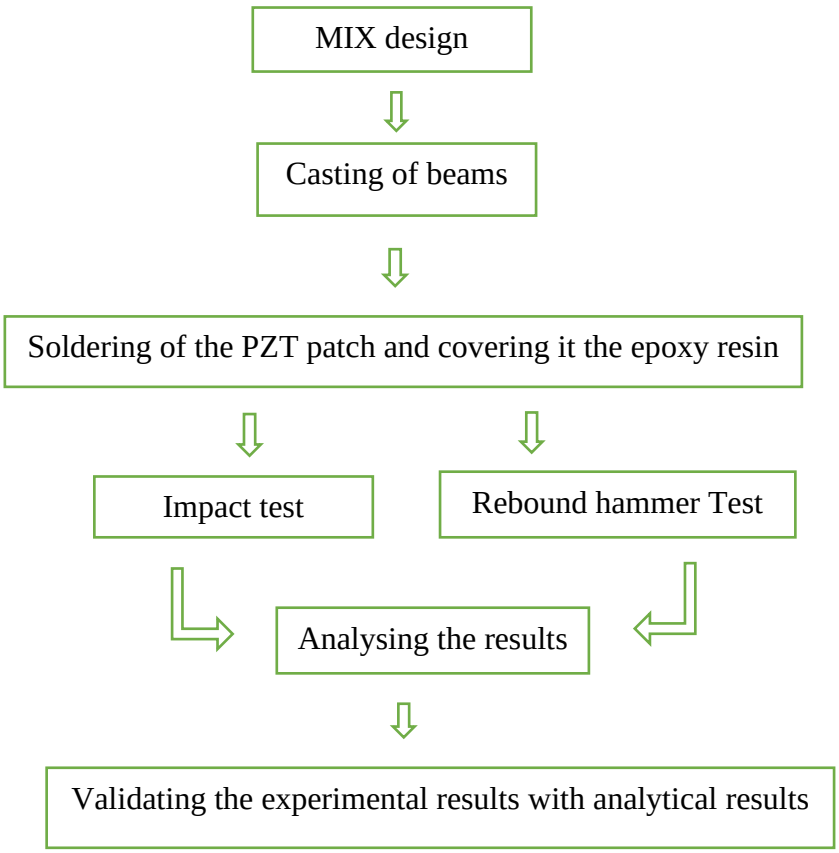


**Fig. 3.1** Flow chart of methodology

## 3. 3 EXPERIMENTAL WORK

The procedure followed for experimental work is explained in detail in the following section. The different instruments used for the experiment and the tests done are elaborated by specifying the conditions followed.

### 3.3.1 Piezo electric sensors

Piezo electric sensor are a kind of sensor which can convert any change in physical parameter like strain or acceleration into electric charge. The PZT patches are very sensitive, thin and brittle materials which has to be taken care of while using. The patches

used for this experimental work was of dimension 10 x 10 mm with a thickness of 0.2 mm as shown in Fig. 3.2 and properties of the PZT patch is given in Table 3.1.

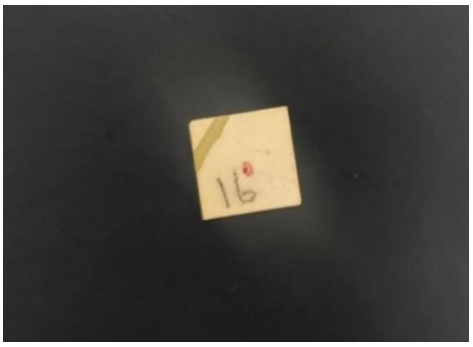

**Fig 3.2** PZT Patch

**Table 3.1** Properties of piezo sensors

| **Property** | **Value** |
|---|---|
| $d_{31}$ , piezoelectric strain coefficient | $-2.74\ X10^{-10}$ C/N |
| $d_{33}$ , piezoelectric strain coefficient | $5\ X10^{-10}$ C/N |
| $\overline{Y^E}$ , the Young's modulus | $5.5\ X10^{10}$ N/m |
| h ,thickness of PZT patch | $2\ X10^{-4}$ m |
| $\overline{\varepsilon_{33}^T}$,electric permittivity of the patch | $3.01\ X10^{-8}$ F/m |

.$\overline{Y^E}$ is the Young's modulus and $\bar{\varepsilon}_{33}^{T}$ is the electric permittivity of the patch, l and h are length and thickness of PZT patch , $d_{31}$ and $d_{33}$ is the piezoelectric strain coefficient

The small division in the patch separates the positive side and negative side of the sensor. They have to be taken care with utmost precision because of their high sensitivity to any sort of disturbance.

This PZT patch is then soldered with soldering wire in both the positive and negative side by fixing the polarity of the wire and continuing with the same throughout the whole

experiment as well as shown in Fig. 3.3. After soldering, the PZT patches are tested using LCR meter to make sure that the patch is still working by analysing the curves of the admittance signature. The frequency v/s susceptance graph will go down, if the PZT patch is not working. This is one way of ensuring that the PZT patches are in working condition and that one hasn't damaged it while soldering.

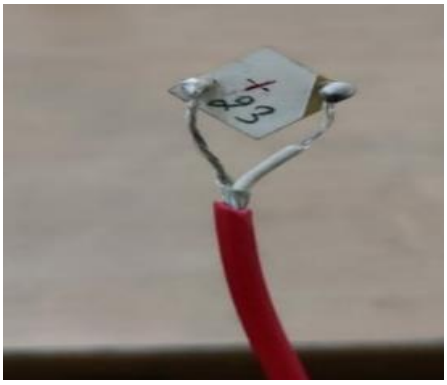

**Fig. 3.3** Soldered PZT patch

Once PZT patches are soldered, it is then covered with epoxy adhesives, here araldite was used as the adhesive. This is done to ensure that the sensor is protected from any disturbance that might happen during the casting or vibration. For this, a plastic mould was used and it was made sure that the patches were in the middle and evenly coated. Once it is dried, the plastic mould is removed and the sensor are ready for casting as shown in Fig. 3.4.

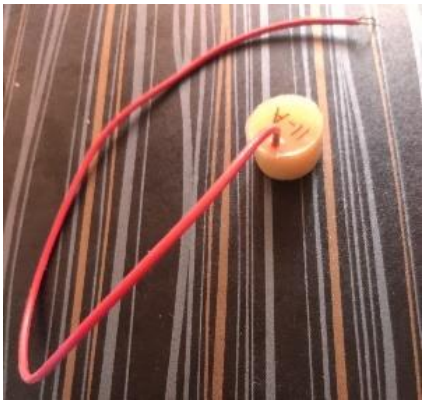

**Fig.3.4.** PZT patch covered with epoxy

### 3.3.2 Casting of beams

M30 grade concrete has been used for the casting of beams. Mix design was done in accordance with IS:10262 (2009) . Portland pozzolana cement or PPC was used for the concrete. Compressive strength was tested to confirm the ratio. During the casting procedure, the mould is marked to where the sensor has to be placed i.e., the centre of the mould and once the mould is filled halfway with the concrete, the sensor that is covered in epoxy resin is placed in position as shown in Fig. 3.5 and the rest of it is filled as shown in Fig. 3.6. The beams are demoulded after 24 hrs and placed in a curing tank for 28 days to gain strength. After 28 days, the beams are taken out and the test was carried out.

**Fig. 3.5** Placing the PZT patch in the concrete

**Fig. 3.6** Casting the beams

### 3.3.3 Instruments used for the testing

Two different types of instruments are used for the experimental work. LCR meter for recording the admittance signature and oscilloscope for measuring the voltage. The features of these instrument are explained in the following section.

#### 3.3.3.1 *LCR meter*

LCR meter is an instrument used for measuring the impedance of a material. Impedance is the measure of resistance to the electric flow. In this study, Keysight technologies, E4980A LCR meter is used. This LCR meter offers excellent speed, accuracy and versatility. The frequency range offered by this instrument is from 20 Hz to 2MHz. It even provides a LAN,USB and GPIB interface to copy the data recorded. It is very light weight and easy to use. Some properties of the Keysight E4980A LCR meter is mentioned in the Table 3.2 below.


**Fig 3.7** LCR meter

**Table 3.2** Features of the Keysight LCR meter

| | |
|---|---|
| Frequency | 20Hz to 2 MHz |
| Signal level | 0 to 2 Vrms/0 to 20 mArms<br>0 to 2 Vrms/0 to 100 mArms[1] |
| DC source | ±10 V[1] |
| Remote control | LAN ,USB,GPIB |
| Basic accuracy | 0.1% for Short<br>0.05% for Medium/long |
| Storage | Internal/ USB memory |
| Weight | 5.3 Kg |

### 3.3.3.2 *Oscilloscope*

An oscilloscope is an electronic device which displays the varying electronic voltages graphically. The oscilloscope used for this experiment was Tektronix TBS2000B digital oscilloscope. It has 4 analog channel models and a 5 million point record length. The TBS2000B series is easy to operate and gives accurate results.


**Fig. 3.8** Oscilloscope

### 3.3.4 Different types of tests done on the specimen

Impact test, where an impulsive dynamic load that acts in a very short time is carried out for analysing for the damage detection property of a structural element under impact load. On the same beams, before and after impact, one of the common NDT techniques called the rebound hammer test has also been done to compare them.

#### 3.3.4.1 *Impact Test*

Impact load analysis has a wide range of application in Civil Engineering. It helps in understanding the impact resistance of a structure which is the ability to absorb and dissipate energy without causing damage to the structure due to an impulsive dynamic load which occurs in a short time. Impact load arises in various situation such as a structure when is hit by a vehicle, a marine structure subjected to ice load as an impact, aircraft crashes, accidental drop weights and terrorism attacks

A spherical ball of 5 kg in weight has been used as the impact ball and is dropped from a height of 3m. The height and weight of the ball was taken in accordance to the criteria mentioned in drop weight test mentioned in ACI 544 – 2R code with slight differences. A vertical pipe was designed to make sure that the point of impact after dropping the ball is centre. The voltage has been monitored at the time of the impact with the help of an oscilloscope. Before and after each impact, the altered admittance signature from the PZT patch has been recorded with the help of an LCR meter.

#### 3.3.4.2 *Rebound hammer test*

Rebound hammer test is one of the non- destructive technique evaluation which gives a rapid value of compressive strength of the concrete. This method is very easy and convenient to use. In order to test, the plunger is pushed into the concrete perpendicular to its surface, and the force causes the latch to release and makes an impact on the

concrete. The output of the rebound hammer is known as rebound number and this is related with the surface hardness of the concrete. The hardness of the concrete is then again related to the compressive strength . The relation between rebound number and compressive strength s given by EN 13791 - 2007, and it is given by equation (3.1) ,

$$f_r = 1.73\ X\ R - 34.5 \tag{3.1}$$

Where, $f_r$ is the compressive strength and the R is the rebound number


**Fig. 3.9.** Rebound hammer

### 3.4 EXPERIMENTAL SETUP

The setup used for the impact test is as shown in Fig. 3.10. The vertical pipe has been used to guide the ball that is being dropped from a height of 3m. The impact ball is a steel ball of 13 cm diameter and weighs 5 kg and is tied with the help of a rope for dropping as shown in Fig. 3.11. One end of the LCR meter is connected to the laptop to record the data and save it for future references and the other end is connected to the PZT patch inside the sample to obtain the admittance signature as shown in Fig. 3.12 before and after impact. The oscilloscope records the voltage during the impact.

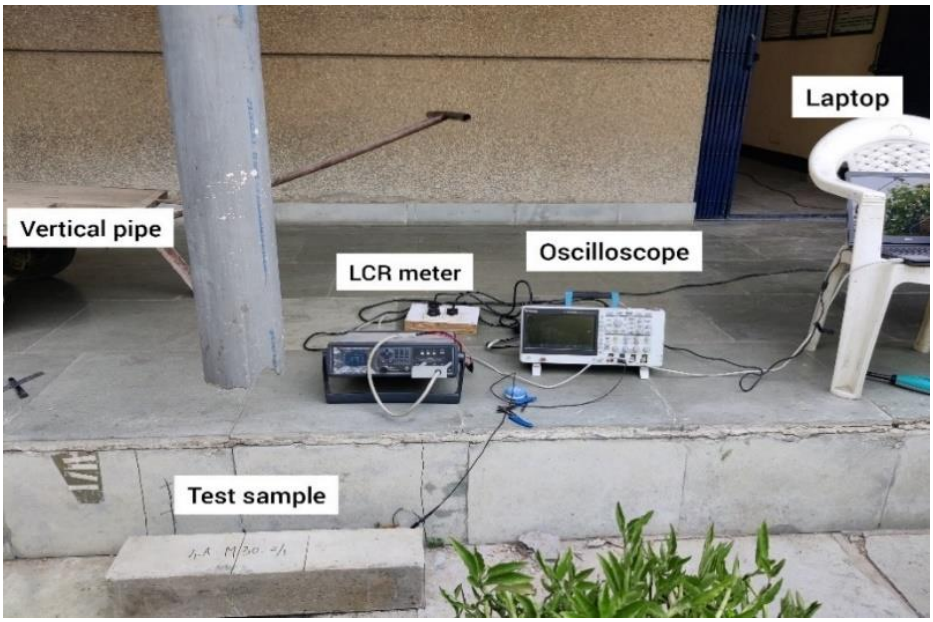


**Fig. 3.10** Experimental setup

**Fig. 3.11** Impact Ball

**Fig. 3.12** Connection point

### 3.5 ANALYTICAL STUDY

The experimental study has been simulated analytically by using ANSYS software to do finite element analysis and the strain value has been used to compare and validate the experimental work.

#### 3.5.1 Ansys – Finite element analysis

Finite element analysis can solve structural problems and evaluate the capability for service, failure analysis, fatigue life or performance design optimization. In the present study, FEM has been done using the explicit dynamics module in ANSYS software.

Explicit dynamics is a system component of the ANSYS workbench. It can be used to simulate responses of highly transient, nonlinear physical phenomena like drop test and high speed impact. The steps involved in finite element modelling in ANSYS are:

- Adding material properties
- Creating the model geometry
- Create meshing and body interaction
- Analysis and data collection

### 3.5.2 Meshing of the model

After the geometry of the model was created as per the dimension of the beam 700 x 150 x 150 mm , the next step is to assign the materials to the elements and create meshing. Meshing is the process of diving a geometric shape into thousands of little pieces to properly define the shape of the object and to give a more accurate analysis and result. For this, a meshing of 20 mm was done for the model as shown in Fig. 3.13 as per the mesh convergence study .

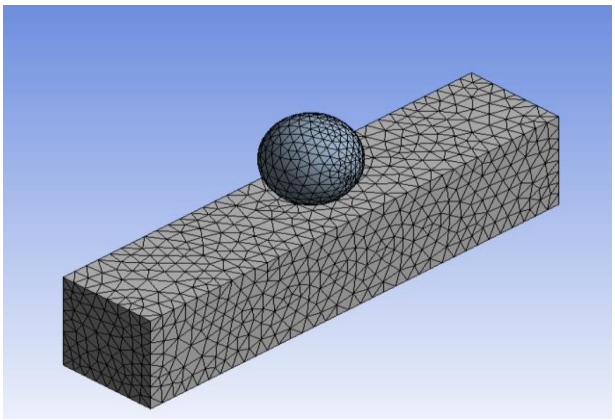

**Fig. 3.13** Meshing

### 3.5.3 Body Interaction

The body interaction folder under connections is used to define a global connection option for explicit dynamics. They are used to give surface to surface contact between two

different materials[7]. They body interactions available are mainly bonded, frictional, frictionless and reinforcement. In the present study, frictional body interaction has been assigned to the model.

### 3.5.4 Velocity

The two main values important in creating an impact load in ANSYS is velocity and end time. Impact testing are divided into two types based on velocity namely, low velocity impact by a large mass and high velocity impact by a small mass[19]. Here low velocity impact (drop weight test) is used. Once the meshing and body interaction has been assigned, end time is provided under the initial analysis option. In this study ,the end time given was 0.35 milli-s. This value was chosen as the maximum deformation for the impact was obtained during this end time. The velocity determines the force of impact. To find the velocity, equation (3.1) was used.

$$v = \sqrt{2gh} \tag{3.1}$$

where $h$ is the height of impact.

# CHAPTER 4

# RESULTS AND DISCUSSION

## 4.1 GENERAL

Impact load is an impulsive dynamic load which occurs in a short time. Impact resistance of a structure is the ability to absorb and dissipate energy without causing damage to the structure. Embedded PZT patches are used in order to quantify this damage and understand the ability of these sensors in damage detection.

### 4.1.1 Admittance signature

The obtained admittance signatures were compared for each impact to understand the deviation of it after impact. The admittance signature is the unique signature of the structure with all the properties. After the impact, the structural properties undergo some changes and hence the admittance signature get altered. This alteration indicates damage. In this study, admittance signature was measured before and after impact with the help of a LCR meter. Measurements were taken for a frequency range of 30-600 KHz and the admittance signature was recorded.

### 4.1.2 Damage indices

Three different damage indices namely, RMSD and MAPD index have been used to quantify the damage. It is a technique used to calculate the amount of deviation of the admittance signature statistically after impact i.e., when the damage has occurred in the structure with the baseline admittance signature. RMSD or root mean square deviation index is the most commonly used damage index for health monitoring. In the equations (4.1) and (4.2), $x_i$ is the real part of the impedance signal (conductance) of the baseline signature i.e., before impact and $y_i$ is the real part of the impedance signal after the

damage has occurred. N indicates the total number of signatures. $\sigma_x$ and $\sigma_y$ represents standard deviation and $\bar{x}$ and $\bar{y}$ is representing the mean of the values.[21]

$$RMSD\ \% = \sqrt{\frac{\sum_{i=1}^{i=N}(y_i - x_i)^2}{\sum_{i=1}^{i=N} x_i{}^2}}\ X\ 100 \tag{4.1}$$

$$MAPD\ \% = \frac{1}{N}\sum_{i=1}^{N}\left|\frac{y_i - x_i}{x_i}\right|\ X\ 100 \tag{4.2}$$

### 4.1.3 Strain of the PZT

A relation was developed between the voltage generated across the PZT and the strain developed in the host structure by shanker et al [14] and it is given as:

$$V = \left(\frac{d_{31}\overline{Y^E}h}{\overline{\varepsilon_{33}^T}}\right)S_1 \tag{4.3}$$

here, V is the output voltage. From the above equation, strain can be calculated by substituting the value of V that is obtained by using an oscilloscope and connecting it to the PZT patch.

## 4.2 COMPARISON AND VALIDATION OF STRAIN

The strain of PZT after impact is found out with the help of voltage that is obtained from the oscilloscope recording from the sensor. This strain is compared with the strain obtained from doing finite element modelling in ANSYS by simulating the same impact analysis.

### 4.2.1 Validation of impact loading from literature

Analytical results from the literature Partheepan et al (2019 ) was used for validating the FEM model [11]. In the literature, an RC slab was analysed with dimension 500x600x50 mm with the support condition as opposite sides having simply supported condition. Deformation values for impact analysis with three different values were analysed and results obtained along with the percentage difference is shown in Table 4.1.

**Table 4.1** Comparison of deformation from literature and software

| Velocity (mm/s ) | Deformation as per literature (mm) | Deformation obtained from software (mm) | Percentage difference (%) |
|---|---|---|---|
| 1154 | 0.49 | 0.50 | 2.4 |
| 2308 | 0.99 | 1.003 | 1.3 |
| 3462 | 1.4 | 1.47 | 4.8 |

From Table 4.1 , it is observed that the deviation or % error from the value in literature Partheepan et al (2019) [11] is only 1 – 5%. After the validation part was successful for finite element analysis for impact load, this same procedure is followed for the analytical study in this paper.

### 4.2.2 Analytical model

The finite element modelling is done in the explicit dynamics module in ansys software. Beam of size 150x150x700mm is modelled with a 13cm diameter steel ball as an impactor is designed.

The force of impact is imparted through velocity which is calculated from height using the equation (3.1) . The velocity input is 7003 mm/s. The end time chosen according the Partheepan et al is 0.92 milli sec [11]. Normal strain in X direction is calculated as the equation derived for strain is in X direction. Since the PZT is embedded into the concrete structure in the centre position, in the software also, the strain obtained at the centre position has to be considered. This is because , the value of strain obtained from the numerical calculation through voltage is of the PZT patch, which is placed in the centre position of them beam and not the strain on the surface of the beam . Hence the obtained strain from software analysis is $2.4\ X\ 10^{-5}$ at the centre position as shown if Fig. 4.1.

Here normal strain in X- direction is considered as the numerical study is based on direction and it related to the X- direction.

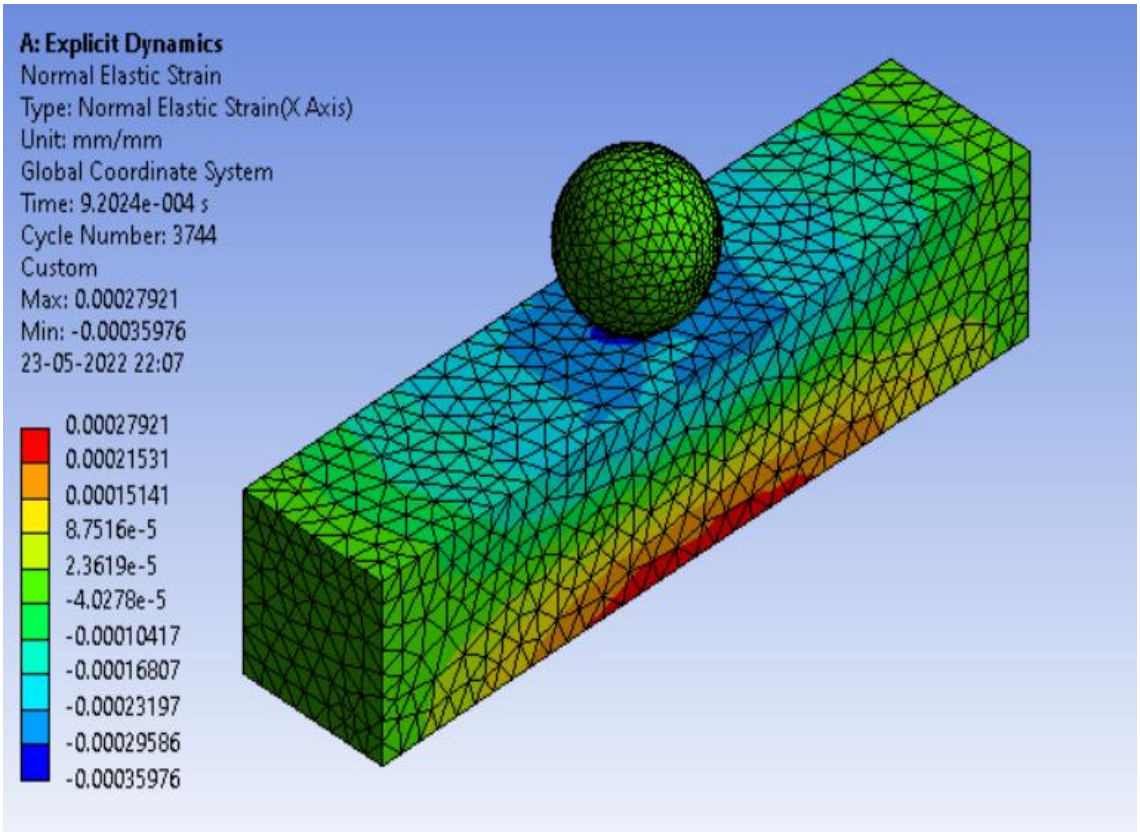


**Fig. 4.1** Value of strain from ANSYS

### 4.2.3 Numerical calculation

As per the relation developed between voltage and strain, voltage is given by equation (4.5) and this can be rewritten to get strain as equation (4.6)

$$S_1 = \left(\frac{\overline{\varepsilon_{33}^T}}{d_{31}h\overline{Y^E}}\right)V \tag{4.6}$$

Since, the PZT patch is embedded in the concrete beam, $d_{31}$ is substituted with $d_{33}$ [1] and from Table 3.1, the properties of the piezo sensors are substituted in the above formula and peak voltage obtained from the oscilloscope which is 4.726 V from Fig. 4.2 is substituted to obtain the value of strain as:

$$S_1 = \frac{3.01X10^{-8}}{5\ X\ 10^{-10}\ X\ 2\ X\ 10^{-4}\ X\ 5.55\ X\ 10^{10}}\ X\ 4.73 = 2.5\ X\ 10^{-5}$$

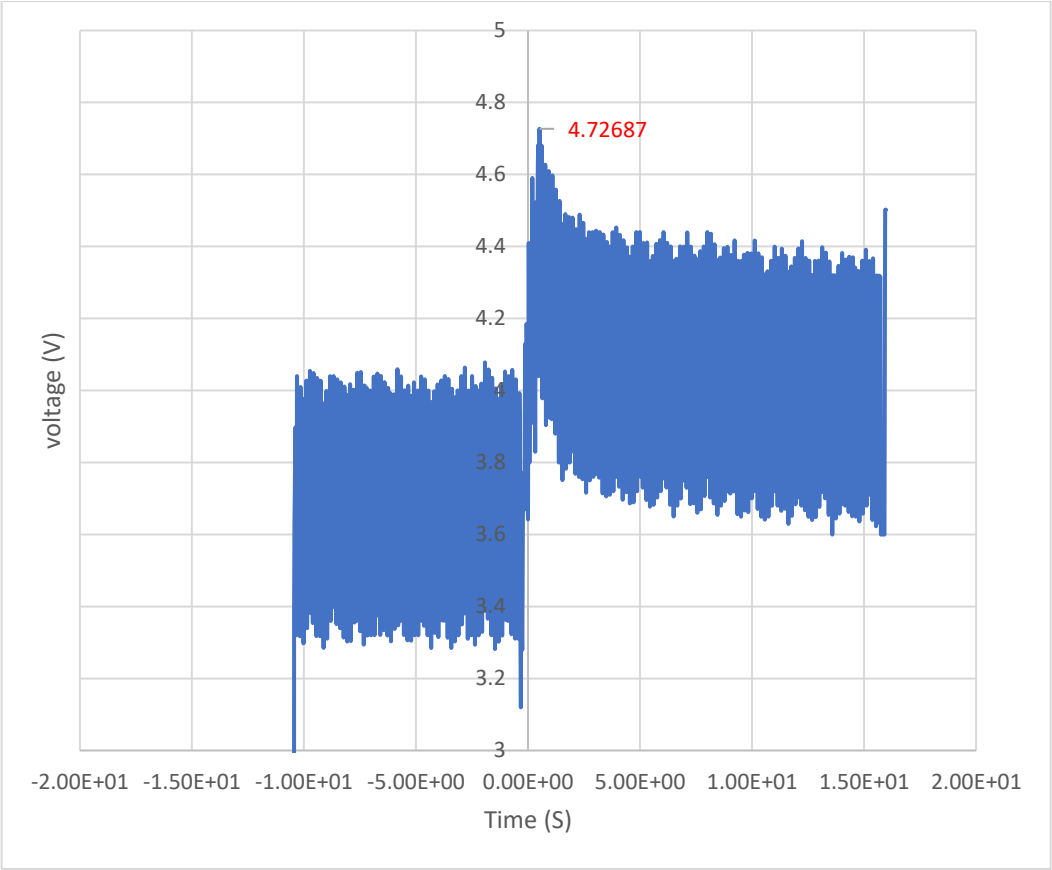


**Fig. 4.2** Peak value of voltage

**Table 4.2.** Comparison of Strain from experiment and software analysis

| | |
|---|---|
| Strain from experimental analysis | $2.5\ X\ 10^{-5}$ |
| Strain from software analysis | $2.4\ X\ 10^{-5}$. |
| Percentage difference | 4 % |

The two value of strain, experimental and analytical, has only a percentage difference of 4% which is within the acceptable percentage error and this small difference might be due to the extensive temperature at Delhi while the casting and experiment was performed which might have affected the concrete properties. Hence the validation of strain with finite element modelling has been successfully performed.

## 4.3 PARAMETRIC STUDY

Three different parametric study has been carried out to understand how the PZT patches help in detecting damage due to impact load. The three different parameters considered are as follows:

- Height of impact
- Grade of concrete
- Position of the sensors

### 4.3.1 Height of impact

Parametric study of height of drop if the impactor was studied at 2 heights , namely 2.5m and 3m for M30 grade of concrete with embedded sensor at the centre. The crack pattern is shown in Fig. 4.3 .The admittance signatures and the damage indices were compared and it was observed that the peak of the signature is increasing before and after impact.

**Fig. 4.3** Crack due to impact height of 3m and 2.5 m respectively

#### 4.3.1.1 *Admittance signature comparison for different height of impact*

The signature has been compared for before and after impact and the graph is shown in Fig. 4.4.

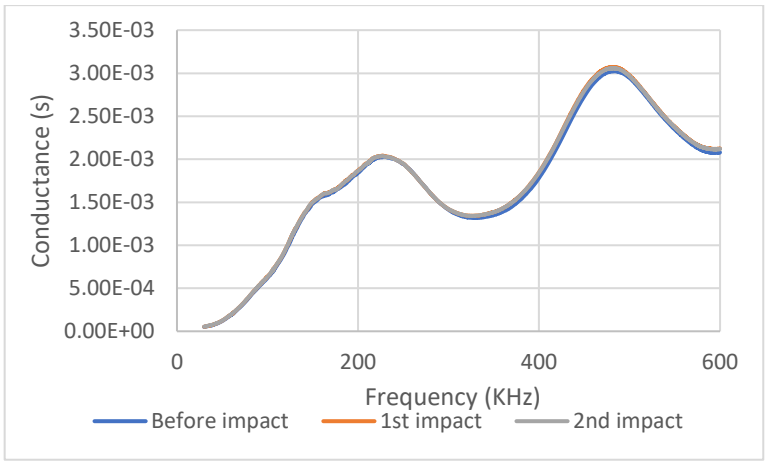


**Fig. 4.4** Conductance v/s frequency for impact height of 3m

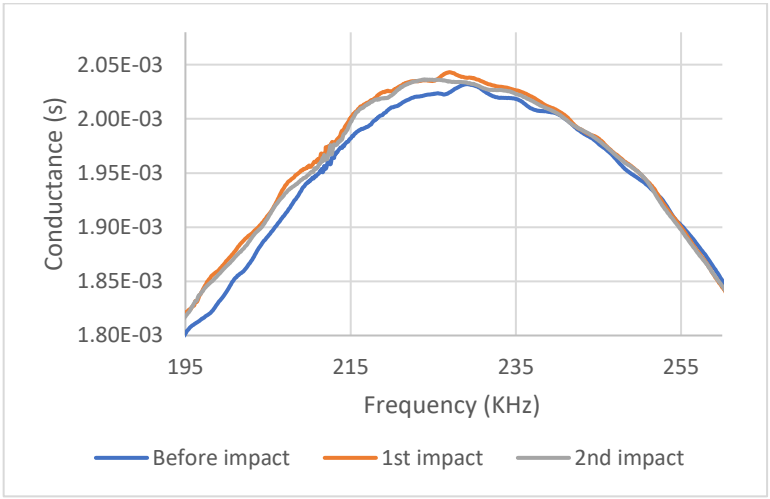


**Fig. 4.5** Enhanced peak of signature for impact height of 3m

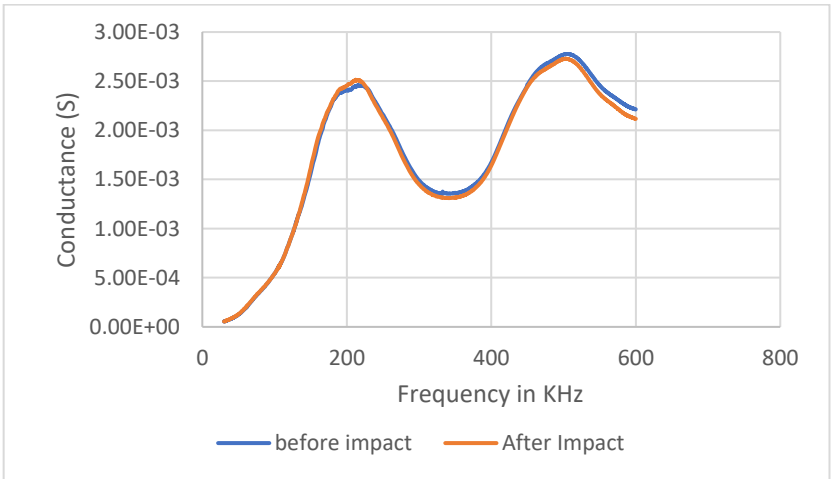


**Fig. 4.6** Conductance v/s frequency for impact height of 2.5m

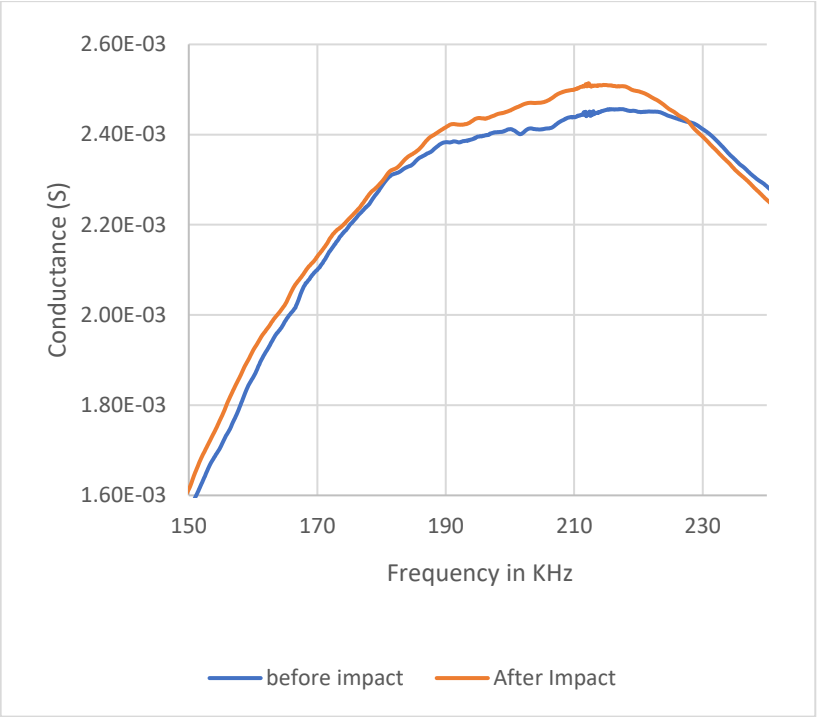


**Fig. 4.7** Enhanced peak of signature for impact height of 2.5m

From Fig 4.5 and 4.7 , it can be observed that the admittance signature is changing before and after impact with the peak value increasing which indicates that there is an increase in damage in the structural element after impact .A comparison of peak value for both height is shown in Table 4.3.

**Table 4.3** Comparison of peak value of conductance at different heights of impact

| Impact number | Peak value of conductance | |
|---|---|---|
| | At height 3m | At height 2.5m |
| 0 | $3.02 \times 10^{-3}$ | $2.73 \times 10^{-3}$ |
| 1 | $3.09 \times 10^{-3}$ | $2.78 \times 10^{-3}$ |
| % Difference | 2.29% | 1.82% |

The percentage difference for the peak value for height 3m which is 2.29 % is much more compared to 2.5m, which is around 1.82% . This is because the force of impact is very high when the ball is dropped from a height of 3m, hence the damage is more and the

signature deviates to a higher peak leading  a greater percentage difference for the peak value of conductance .

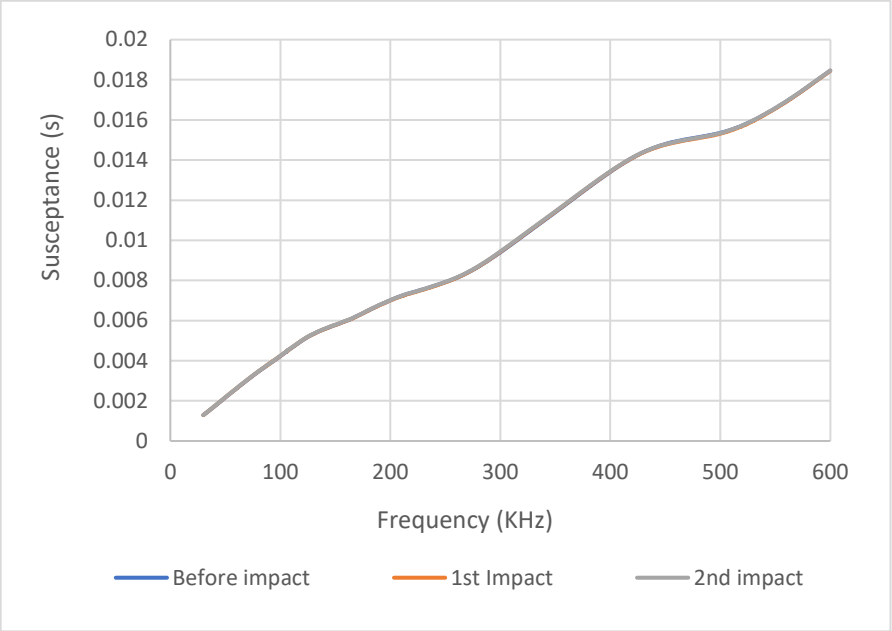


**Fig. 4.8** Susceptance v/s frequency for impact height of 3m

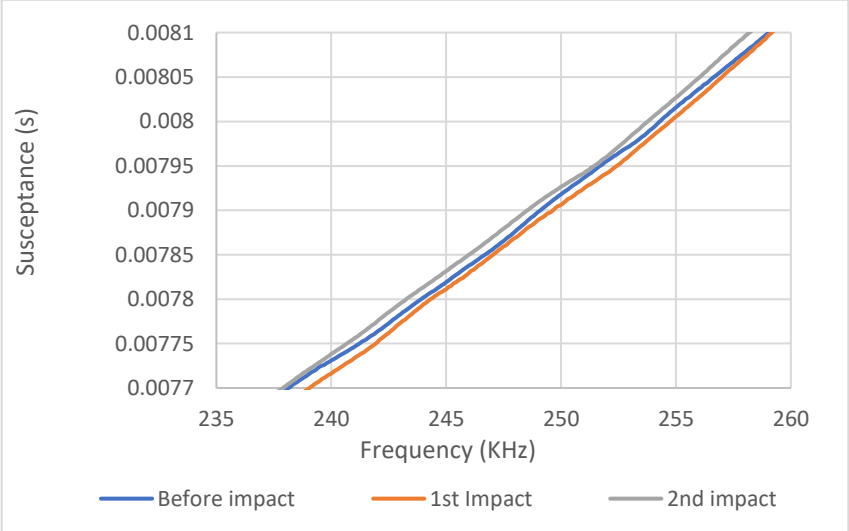


**Fig. 4.9** Enhanced peak of susceptance signature for impact height of 3 m

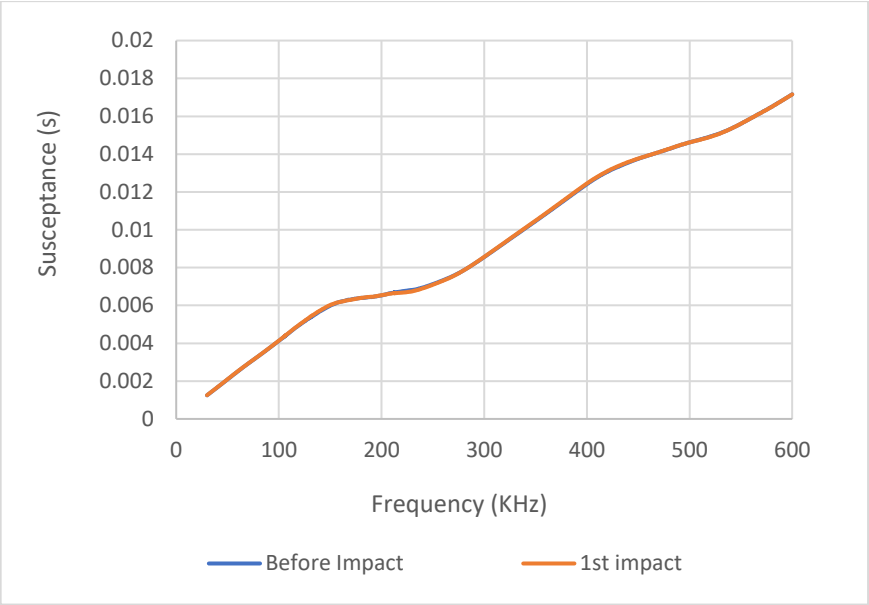


**Fig. 4.10** Susceptance v/s frequency for impact height of 2.5m

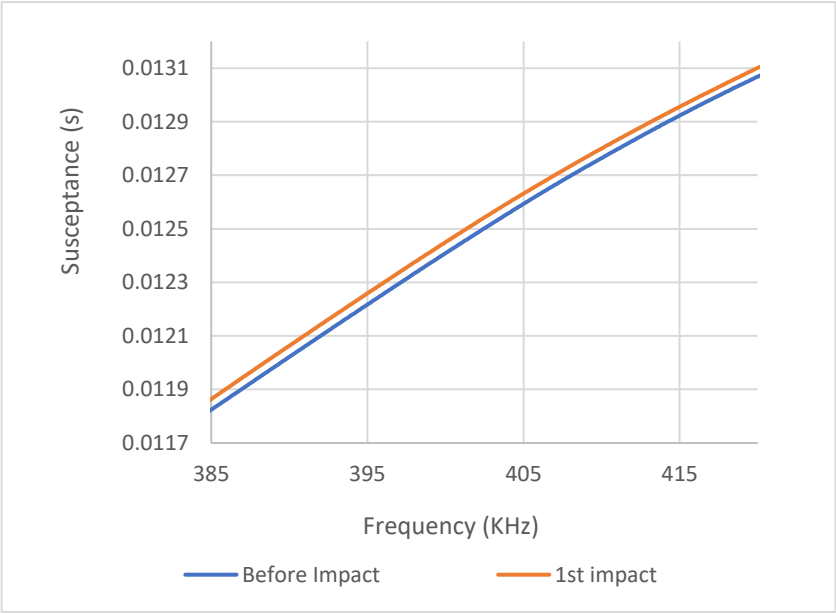


**Fig. 4.11** Enhanced peak of susceptance signature for impact height of 2.5 m

The straight line in the susceptance v/s frequency graph indicates that the PZT patch was in working condition and intact to the structure.

#### 4.3.1.2 *Damage index comparison for different height of impact*

The deviation of signature has also been statistically found out using the 2 indices, namely RMSD and MAPD for both the heights.

**Table 4.4.** Comparison of damage indices for different height of impact

| Height (m) | RMSD (%) | MAPD(%) |
|---|---|---|
| 3m | 5.55 | 2.18 |
| 2.5m | 1.32 | 1.76 |

It can be observed that as height increases, force of impact increases which leads to increased damage due to impact, hence it can be seen that both damage indices show an increase in the value for 3m height i.e., a linear relationship can be observed in the value of damage indices from 2.5m height to 3m height.

### 4.3.2 Grade of concrete

M30 and M25 grade of concrete was taken for comparing the damage detection properties of PZT patch under impact load for different grades of concrete. The impactor was dropped from a height of 2.5m . The crack pattern obtained for M25 grade of concrete is shown Fig 4.12.

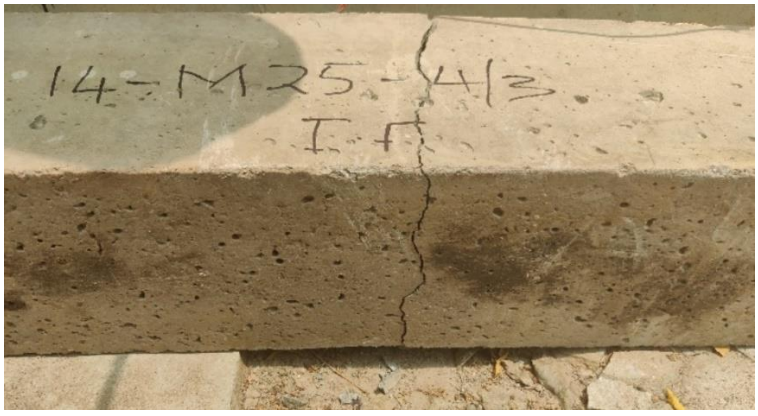


**Fig. 4.12** Crack patter for M25 grade of concrete

The admittance signature graphs for M30 grade at 2.5 m height is shown in Fig. 4.6,4.7,4.10 and 4.11. The admittance signatures for M25 grade is shown in Fig 4.13.

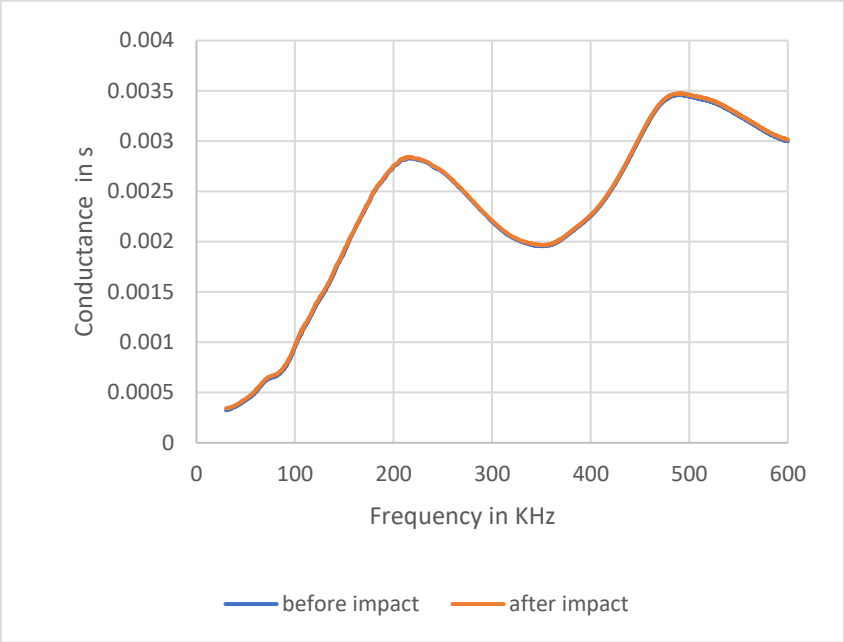


**Fig. 4.13** Conductance v/s frequency for M25 grade at 2.5 m height

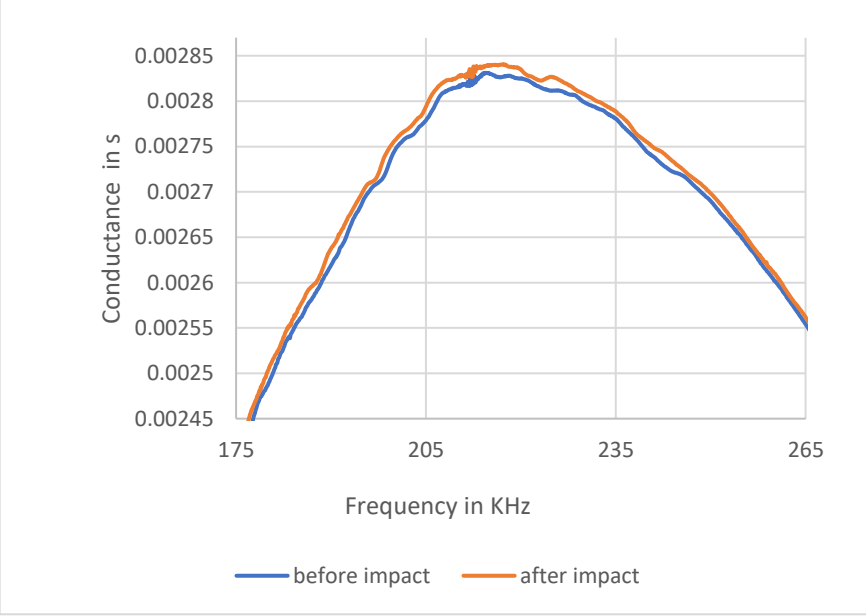


**Fig. 4.14** Enhanced peak of signature for M25 grade

**Table 4.5** Comparison of peak value of conductance for different grade of concrete

| Impact number | Peak value of conductance | |
|---|---|---|
| | M30 grade | M25 grade |
| 0 | $2.73 \times 10^{-3}$ | $3.458 \times 10^{-3}$ |
| 1 | $2.78 \times 10^{-3}$ | $3.474 \times 10^{-3}$ |
| % Difference | 1.82% | 5.44% |

From the peak values obtained in Table 4.5, it can be concluded that M25 grade of concrete is affected more due to impact as the percentage difference obtained for the peak value after impact is much more for M25 which is 5.44 % compared to M30 grade which is 1.82 % only. This indicates that M25 grade of concrete has less strength compared to M30 which is why more damage is occurred in M25 grade concrete beam.

#### 4.3.2.1 *Damage index comparison for different grades of concrete*

The deviation of signature has also been statistically found out using both indices, namely RMSD and MAPD for both the grades of concrete.

**Table 4.6.** Comparison of damage indices for different grades

| Grade | RMSD (%) | MAPD(%) |
|---|---|---|
| M25 | 6.064 | 3.99 |
| M30 | 1.32 | 1.76 |

For different grades of concrete , it can be seen that it also follows a linear relationship from M30 to M25, i.e., there is a decrease in value from M25 to M30, with a percentage difference of 4.744% for RMSD value and 2.23% difference in MAPD value. This is because M30 grade of concrete has higher strength compared to M25, which causes less damage due to impact compared to M30.

### 4.3.3 Position of the PZT patches

For all other parameters, the PZT patch has been embedded in the centre of the beam and the testing has been done. In order to study the effects of position of the sensors, a different positioning was done where, 2 PZT patches were placed at 1/3$^{rd}$ distance from the sides as shown in Fig 4.15.

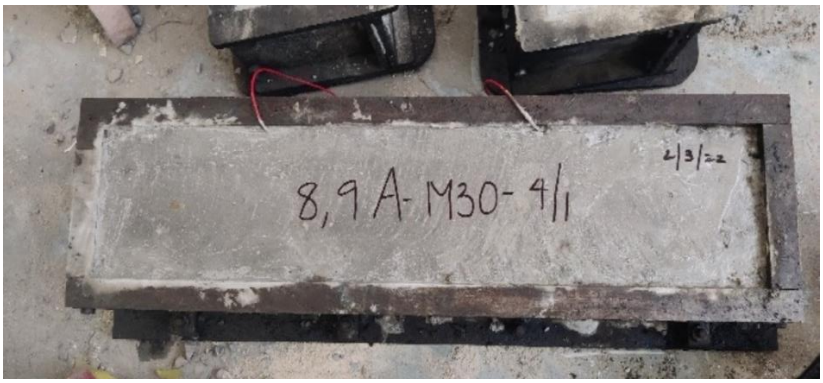


**Fig. 4.15** Sensors at 1/3$^{rd}$ distance from the edge on both sides

The height of impact was considered as 2.5m height and the position of impact was at centre. The admittance signature was taken for both the sensors before and after impact with LCR meter separately. The signature is shown below in Fig 4.16.

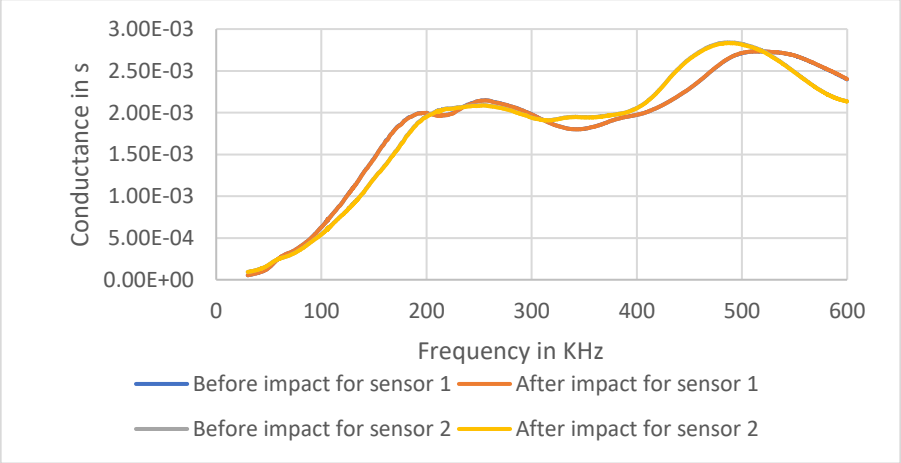


**Fig. 4.16** Conductance v/s frequency for PZT patch at 1/3$^{rd}$ distance from the ends

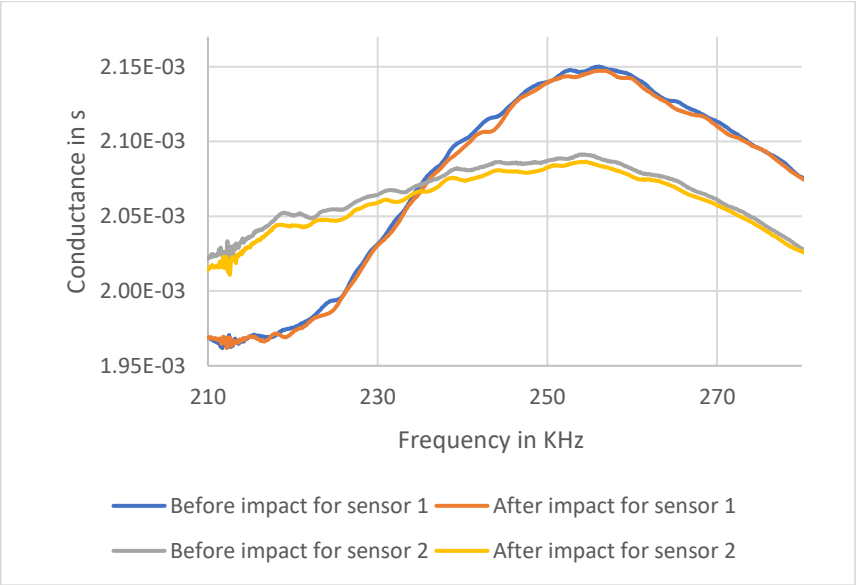


**Fig. 4.17** Enhanced peak of signature for PZT patch at 1/3$^{rd}$ distance from the ends

From the admittance signature , it can be seen that there is a change in the pattern followed before and after impact compared to all other parameters. The signature after impact is having a peak lower compared to before impact. Since the sensors are placed at 1/3$^{rd}$ distance from the ends, the damage due to impact at centre has not been properly recognised by the sensors compared to how the sensors placed in the centre position recorded the signature after impact. This is because, the sensors placed near the edges are not near the position of impact and this might have affected the pattern followed but it can be observed that there is still a difference in the admittance signature recorded before and after impact, which indicates that the damage is still being recorded. .

**Table 4.7** Comparison of peak value of conductance for different position of sensors

| Impact number | Peak value of conductance | | |
|---|---|---|---|
| | Sensors at centre | Sensors at 1/3$^{rd}$ distance at 2 edges | |
| 0 | 2.73 x $10^{-3}$ | 2.73 x $10^{-3}$ | 2.84 x $10^{-3}$ |
| 1 | 2.78 x $10^{-3}$ | 2.74x $10^{-3}$ | 2.83x $10^{-3}$ |
| % Difference | 2.29% | 0.36% | 0.46% |

From Table 4.7, it can be seen that the percentage difference between the peak value before and after impact for sensor placed at centre is more by 1.83 – 1.93% compared to the sensors placed at 1/3rd distance from edges indicating that sensors placed at centre records the impact damage better.

#### 4.3.3.1 *Damage index comparison for different positioning of sensors*

The deviation of signature has also been statistically found out using both the indices, namely RMSD and MAPD for both positions of sensors.

**Table 4.8.** Comparison of damage indices for different position of sensors

| Position | RMSD (%) | | MAPD(%) | |
|---|---|---|---|---|
| 1/3rd distance | Sensor 1 | Sensor 2 | Sensor 1 | Sensor 2 |
| | 1.118 | 0.6266 | 0.132 | 0.279 |
| Centre | 1.32 | | 1.76 | |

Both RMSD and MAPD value are having a linear relationship between the two parameters before and after impact. When sensors are embedded near the edges, the value is coming to be less even though all other parameters are same is because, the PZT are more efficient in detecting damages when they are placed near to the impact position.

## 4.4 FLEXURAL TEST

Flexure strength indicates the maximum force or stress that a beam can withstand without bending. It is an indirect measure of the tensile strength of beam. As per IS 516, flexure strength is measured by calculating modulus of rupture $f_b$ by the equation given below.

If a is greater than 20 cm for 15 cm specimen,3

$$f_b = \frac{Pl}{bd^2} \tag{4.7}$$

And if a is less that 20cm and greater than 17 cm for 15 cm specimen,

$$f_b = \frac{3Pa}{bd^2} \tag{4.8}$$

Where "a" is the distance between the line of fracture and nearest support, p is the load at failure, $l$ is the support length , b is the width of the specimen and d is the failure point depth [24].

In this study, Flexure test was done with the help of a UTM or universal testing machine.

**Fig. 4.18** Universal testing machine

M30 grade and M25 grade of concrete was casted in order to find the flexure strength and do a comparison. The average value of a for M30 beam was obtained as 213 mm and for M25 205mm, hence equation(4.7) is used.

By substituting the value of $l$ = 600mm, b= 150 mm , d=150 mm

**Table 4.9** Average flexural strength

| Grade of concrete | Load at failure (KN) | Flexural strength ($N/mm^2$) | Average Flexural strength ($N/mm^2$) |
|---|---|---|---|
| M30 | 36.9 | 6.56 | |
| | 37.6 | 6.68 | 6.44 |
| | 34.2 | 6.08 | |
| M25 | 27.6 | 4.90 | 4.69 |
| | 26.4 | 4.69 | |
| | 25.3 | 4.49 | |

It can be observed that M30 grade of concrete has high flexural strength compared to M25.

## 4.5 REBOUND NUMBER

Rebound hammer test was also done before and after impact to compare the NDT technique with SHM. The average value of rebound number was taken for comparison in each impact. The rebound number also indicates the quality of concrete as given in Table 3.2. All of the beams has an average rebound number above 40 indicating that all the beams were of good quality concrete.

**Table 4. 10** Rebound number comparison

| Parameter | | Rebound Number | | % difference |
|---|---|---|---|---|
| | | Before Impact | After Impact | |
| Height of impact | 3m | 52.3 | 43.6 | 18.14% |
| | 2.5m | 48.1 | 42.8 | 11.66% |
| Grade of concrete | M30 | 48.1 | 42.8 | 11.66% |
| | M25 | 47.3 | 41 | 14.6% |
| Position of sensor | Centre | 48.1 | 42.8 | 11.66% |
| | $1/3^{rd}$distance from sides | 50.16 | 44.4 | 12.1% |

For different height of impact and grade of concrete, percentage difference is considerably high for higher impact height and lower grade of concrete by 6.48 % and 3% respectively, which further validates the deviation in signature as well, as it follows the same trend for peak value difference i.e., the damage detection by the piezo sensors are also following the same trend followed by the rebound test. Since the parameter where the position of sensor is changed does not affect the property of concrete beam or impact force, the rebound test gives only a slight percentage difference of 0.44 %.

### 4.4.1 Compressive strength from rebound number.

As mentioned in equation (3.1), numerical relationship between compressive strength and rebound number as per EN 13791 - 2007 is given as,

$$f_r = 1.73\,X\,R - 34.5 \tag{4.1}$$

Average value of rebound number is substituted to obtain the compressive strength and it is given in Table 4.10

**Table 4.11** compressive strength from Rebound number

| Parameter | | Rebound Number | | Compressive strength (MPa) | | % difference |
|---|---|---|---|---|---|---|
| | | Before Impact | After Impact | Before impact | After impact | |
| Height of impact | 3m | 52.3 | 43.6 | 55.97 | 40.928 | 31.04% |
| | 2.5m | 48.1 | 42.8 | 48.71 | 39.54 | 20.78% |
| Grade of concrete | M30 | 48.1 | 42.8 | 48.71 | 39.54 | 20.78% |
| | M25 | 47.3 | 41 | 47.32 | 36.43 | 26.06% |
| Position of sensor | Centre | 48.1 | 42.8 | 48.71 | 39.54 | 20.78% |
| | 1/3$^{rd}$distance from sides | 50.16 | 44.4 | 52.27 | 42.312 | 21.05% |

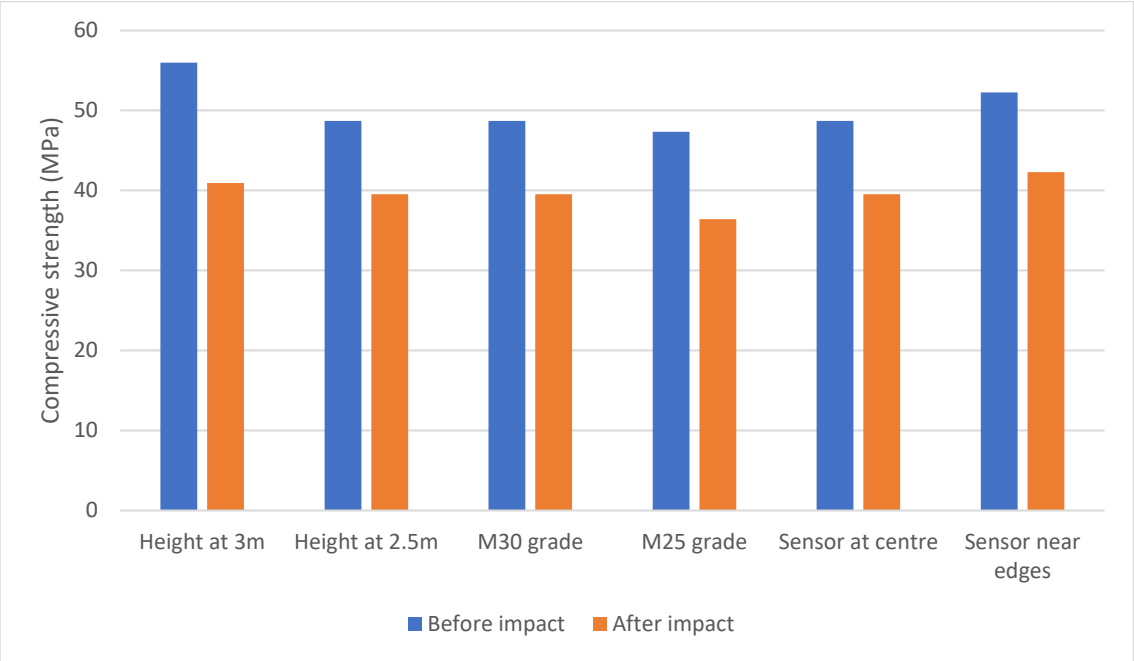


**Fig. 4.19** Comparison of compressive Strength before and after impact

Fig. 4.19 shows the graphical represntation of Table 4.10, and it can be seen that compressive strength is decreasing after impact for all the cases. It can be observed that the same trend is being followed, where for different height of impact, percentage difference in compressive strength before and after impact is higher for 3m height, by 10.26% because the force of impact when the ball is dropped from 3m height is more compared to 2.5 m height, hence more damage is occurred. Similarly, for M25 grade of concrete, it is observed that the percentage difference of compressive strength is more by 5.28% as M25 has less strength to withstand the impact compared to M30. For different position of sensors, the percentage difference in compressive strength is very less by 0.27 % because this parameter does not affect the property or impact force for the beam.

# CHAPTER 5

# CONCLUSION

An experimental study was carried out to understand and study the damage detection capability of piezo sensors under impact load for plain concrete beams using electro mechanical impedance technique. The experimental work was validated with analytical model and parametric study was done to analyse how the PZT patches detect the response of the damages under different conditions .

- From the study, it can be clearly seen that after impact, the sensors have been able to successfully record the damage in terms of stiffness, mass and damping. The deviation of peak in the conductance v/s frequency before and after impact indicates the same.
- The straight line observed in the susceptance v/s frequency graph helps to understand that the piezo sensors embedded inside the concrete beam are intact and in proper working condition. If the sensors got damaged after casting, a declining graph was recorded helping us understand that proper response is not being recorded.
- For the parametric study, height of impact, position of sensors and grade of concrete was varied. In first two cases, there was significant percentage difference in peak value obtained before and after impact which further proves the damage detecting capability of sensors.
- As height of impact was increased , more deviation of signature peak value was observed. This is because as height of impact increases, the force of impact increases and damage due to impact is more.
- Similarly, for lower grade of concrete, the peak value deviated with considerable percentage difference as strength is less compared to the higher grade of concrete.

- But in case of the third parameter, the sensors position was changed by keeping the embedded piezo sensor at $1/3^{rd}$ distance from both sides and this was compared to sensor embedded at the centre. This parameter study showed that, piezo sensors detect more damages when they are placed near the position of impact. Even though the detection capacity of the sensors placed near the edges were low, a deviation of in the response was recorded before and after impact.
- Two different damage indices were also used to quantify the damage occurred before and after impact. A linear relationship was seen for all the three parametric study for RMSD and MAPD index .
- Finite element modelling of the beam with same dimension as used for experimental and same impact condition were modelled and simulated in ANSYS software to validate the experiment. It can be observed that the strain obtained through the software analysis and analytical analysis are matching with only a slight amount of percentage error.
- The flexure test done for measuring the tensile strength of the beams was carried out for M30 and M25 grade of concrete. It can be seen that strength of concrete is more for M30 grade compared to M25.
- Rebound hammer test was done before and after impact and the average rebound number for each parameter is also studied. All the beams have rebound number above 40, indicating good quality of concrete and the rebound test follows the same pattern before and after impact to the deviation in admittance signature. This further helps in validating the ability piezo sensors to detect damages.
- Compressive strength was found out from rebound number as per EN 13791 – 2007 , and it can be seen that for lower grade of concrete and higher impact height, the

percentage difference in compressive strength is more since damage occurred is more. This also follows the same patter of decreasing compressive strength after impact.

## FUTURE SCOPE OF WORK

The embedded piezo sensors are very well covered and protected from external environmental factors. Even after impact test, the sensors were still attached to the concrete without any damage. Very few journals have discussed reusability of these piezo sensors. Hence as future scope of work, the reusability aspect of these piezo sensors after impact can be explored. The present study only dealt with plain concrete beams, hence this can be extended to study the response of piezo sensors under impact load for reinforced structural members.

# REFERENCES


[1] A. Dixit and S. Bhalla, "Prognosis of fatigue and impact induced damage in concrete using embedded piezo-transducers" , *sensors and actuators* , 2018 , A 274 , pp 116-131.

[2] A.S.K. Naidu and S. Bhalla , "Damage detection in concrete structures with Smart Piezoceramic transducers ", *SPIE Proc. SPIE Smart Materials, Structures, and Systems* , 2003, vol 5062, pp 684–690.

[3] B. S. Divsholi and Y. Yang, "Comparison of Embedded, Surface Bonded and Reusable Piezoelectric Transducers for Monitoring of Concrete Structures", *Proc. Of SPIE Sensors and Smart Structures Technologies for Civil, Mechanical, and Aerospace Systems*, 2011, Vol. 7981 ,798151-1-10.

[4] C. Liang, F.P. Sun ,C. A. Rogers ,"Coupled electro-mechanical analysis of adaptive material systems-determination of the actuator power consumption and system energy transfer", *J. Intell. Mater. Syst. Struct.,* 1994, vol 5 issue 1, pp 12–20.

[5] C. Pardo De Vero and J. A. Guemes, "Embedded self – sensing Piezoelectric for damage detection", *Journal of Intelligent Material Systems and Structures,* 1998,vol 9 , pp 876-882.

[6] D. Hi, H. Zhu and H. Luo, "Sensitivity of embedded active PZT sensor for concrete structural impact damage detection", *Construction and Building Materials,*2016, vol 111, pp 348–357.

[7] G. Park, H. Cudney and D. Inman, "Impedance-based health monitoring of civil structural components", *J. Infrastruct. Syst.,* 2000 , vol 6, pp 153-160.

[8] H. Gayakwad and J.S. Thiyagarajan, "Structural Damage Detection through EMI and Wave Propagation Techniques Using Embedded PZT Smart Sensing Units", *Sensors,* 2022, vol 22, 2296.

[9] I. Singh , N. Dev , S. Pal . and T. Visalakshi , “Finite Element Analysis of Impact Load on Reinforced Concrete”, *Emerging Technologies and Applications for Green Infrastructure, LNCE,* 2021,vol 203.

[10] N. Kaur, S. Bhalla and S.CG. Maddu ,”Damage and retrofitting monitoring in reinforced concrete structures along with long-term strength and fatigue monitoring using embedded Lead Zirconate Titanate patches”, *Journal of Intelligent Material Systems and Structures*,2018,1–16.

[11] P. Ganesan and S.V.S. Kumar: FE modelling of low velocity impact on RC and prestressed RC slabs, *Structural Engineering and Mechanics*, 2020, vol. 5, , pp. 515–524

[12] P. Negi , T. Chakraborty , N. Kaur and S. Bhalla “Investigations on effectiveness of embedded PZT patches at varying orientations for monitoring concrete hydration using EMI technique”, *Construction and Building Materials*,2018, vol 169 ,pp 489–498.

[13] P. Negi , R. Chhabra , N. Kaur and S. Bhalla , “Health monitoring of reinforced concrete structures under impact using multiple piezo-based configurations”, *Construction and Building Materials,* 2019, vol 222, pp 371-389.

[14] R. Shanker, S. Bhalla, A. Gupta and M.P. Kumar, “Dual use of PZT patches as sensors in global dynamic and local electromechanical impedance techniques for structural health monitoring”, *Journal of Intelligent Material Systems and Structures,* 2011, vol 22, pp1841–1856

[15] S. Bhalla, C.K. Soh, “Structural impedance based damage diagnosis by piezo-transducers”, *Earthquake Engng Struct. Dyn*., 2003, vol 32,pp1897–1916.

[16] S. Bhalla, C.K. Soh, “Structural health monitoring by piezo–impedance transducers. I: modelling ,”*J. Aerosp. Eng.,* 2004, vol 17 (4), pp154–165.

[17] S. Bhalla, C.K. Soh, "Structural health monitoring by piezo–impedance transducers II: applications," *J. Aerosp. Eng*.,2004,vol 17 (4) ,pp 166–175.

[18] S. Fan, S. Zhao, B. Qi and Q. Kong , "Damage Evaluation of Concrete Column under Impact Load Using a Piezoelectric-Based EMI Technique", *Sensors* ,2018, vol *18*(5), 1591.

[19] T.M. Pham and H Hao. : Review of concrete structures strengthened with FRP against impact loading , *Structure*s,2016,vol 7, 59-70.

[20] W. H. Duan , Q. Wang and S. T. Quek , "Applications of piezoelectric materials in structural health monitoring and repair: Selected research examples" , *Materials,* 2010, vol 3, pp 5169-5194.

[21] W. S. Na, D. W. Seo, B.C. Kim and K. T.Park , "Effects of Applying Different Resonance Amplitude on the Performance of the Impedance-Based Health Monitoring Technique Subjected to Damage", *sensors,* 2018, vol 18, 2267

[22] Z. Shu, "Application of piezoelectric materials in structural health monitoring of civil engineering structure", *Chemical Engineering Transactions*, 2017, vol 59, pp 523-528 .

[23] IS 13311 (part 2) : 1992 - reaffirmed 2004, Non-Destructive testing of concrete-methods. of test - part 2 - Rebound hammer.

[24] IS 516 : 1959 - reaffirmed 2004, Method of test for strength of concrete.

[25] EN 13791 – 2007, Assessment of in-situ compressive strength in structures and precast concrete components.